Net shape Functional Parts Using Diode Laser

Tariq Manzur, Chandra Roychoudhuri and Puneit Dua
Photonics Research Center, University of Connecticut
Fahmida Hossain
Massachusetts Materials Research (MMR)
Harris Marcus
Institute of Materials Science, University of Connecticut

Manufacturing processes, such as cutting, drilling, soldering, marking, forming 3D-sintered parts from metal powders and laser vapor deposition, are now well established practices using matured high power lasers like Nd:YAG, CO_2 and Excimer lasers[(1)]. These lasers are bulky, inefficient and expensive. Semiconductor diode lasers, if wavelength is not a disadvantage, hold the potential of creating a major cost/convenience breakthrough in these and other new manufacturing processes such as growing integrated opto-electronics devices etc. They have the potential to initiate a mini industrial revolution because they are compact, have high wall-plug efficiency (50%) and above all, they can be mass produced (like computer chips). It is important to note that almost all laser material processing can be carried out if the intensity available can cover the range from 10^3 to 10^7 W/cm^2. Fortunately, microscopic as they may be, even low power diode lasers emit reliably at 10^6 W/cm^2. The hurdle that needs to be solved is coupling energy from a large number of diodes to obtain high total power without losing much of their inherent brightness and yet keep the system cost low. Price of high power laser diodes have already come down dramatically over the last five years; further reduction is expected as the volume market keeps increasing rapidly. Current commercial devices are mostly of two types: (1) fiber coupled arrays and (2) two-dimensional stacked arrays. We are using both types. We believe, the ultimate high brightness and high total power at low cost will be achieved by 2D array of broad area surface emitting lasers. We will present the results of our various activities using 30W (980 nm, spot size ~ 600 μm), 10 W (860 nm, spot size ~ 50 μm) and 60 W (810 nm, spot size ~ 700 μm) fiber-coupled cw diode laser and 50 W (930 nm spot size ~ 700 μm) free space diode lasers on: (1) fabricating 3D SLS parts directly from metal/ceramic powders using CAD/CAM design, (2) laser assisted selective area vapor phase deposition of amorphous SiC and Si_3N_4-rod, (3) Pb and Ag soldering of simple electronic parts, (4) surface hardening of stainless steel ribbon.

INTRODUCTION

At the University of Connecticut desk-top manufacturing (DTM) test bed uses diode laser to selectively sinter metal/ceramic powders without any polymeric binder at room temperature powder bed and laser assisted selective area metal organic chemical vapor deposition (LASAMOCVD) systems.

At present, solid free form fabrication (SFF) systems using CO_2 and Nd:YAG lasers are more flexible than alternative non-laser SFF technologies, but still have substantial shortcomings that sharply increase the total cost of fabricated parts. Among these shortcomings, existing laser based SFF systems are (a) expensive, with system costs between $300K and $2M and costs of delivered thermal power exceeding $200 per watt, (b) bulky, requiring large floor areas and room volume to accommodate high power CO_2 and Nd:YAG lasers and associated power supplies and cooling systems, inefficient in conversion of electrical energy to thermal energy - CO_2 producing 10-15% conversion of electrical to optical power but then not coupling this optical power efficiently into materials at the long 10.6 μm wavelength, and Nd:YAG producing only 1-3% conversion of electrical to optical power in the inexpensive flash lamp pumped units and achieving 15-20% efficiency only in much more expensive lasers.

Recent advances of diode laser technology makes it possible to deliver thermal energy in compact, efficient, low cost SFF systems, at costs of $30 or less per delivered watt, the cost of fabricated parts would drop rapidly and precision net shape micro parts manufacturers using this new technology would directly be benefited. Table 1 shows a cost analysis of variety of laser-processing systems performed with intensities in the range of 10^3 to 10^8 W/cm^2. Focused diode lasers, despite relatively low output power per stripe (~1W), emit 10^4 to 10^6 W/cm^2, a range suitable for many laser manufacturing jobs[2].

Table 1.Comparison Study of Diode Laser (DL) Mature Conventional Laser Technologies: Relative Performance & Cost

Laser Properties	CO_2	Nd:YAG	Diode Pump Nd:YAG	Excimer	Diode
Wavelength μm	9.6 to 10.6	1.06	1.06	0.19 to 0.35	0.67 to 0.98
Beam	CW Pulsed Single or Multi mode	CW Q-switched Single or Multi mode	CW Pulsed Single or Multi mode	Pulsed Single or Multi mode	CW Modulated Multi mode
Avg. Power	30 W to 10 kW	10 to 500 W	0.1 to 20 W	<150 W	20 to 200 W
Peak Power	10^{8-10} W	10^{8-10} W	10^{8-10} W	10^7 W	NA
Energy Joules	1 to 30	1 to 50	1 to 20	0.1 to 1	NA
Power Density W/cm^2	10^{6-10}	10^{4-9}	10^{3-8}	10^{4-7}	10^{2-6}
Spot size μm	10 to 500	5 to 300	5 to 300	20 to 800	150 to 800
Where Used	Light to Heavy Ind.	Light to Heavy Ind. High Precision	Tele-Com Applicati-on	High Precision	Light Ind.
Toxicity	No	No	No	Yes	No
High Voltage	Yes	Yes	No	Yes	No
RF	Yes	No	No	No	No
Absorption Metal Non-Metal	Small Moderate	Moderate Moderate	Moderate Moderate	Highly Highly	Good Good
Wall Plug-in Efficiency	~ 10%	~1%	~5%	<1%	40 - 50%
Cost of Laser	<$100/W	>$200/W	>$300/W	~$150/W	~$30/W

Sintering Systems

The apparatus used for the present experiment is an extension of a DTM Inc. system[3]. The apparatus includes power delivery system (diode laser), powder delivery system (PDS), oxidation prevention system, laser scan control system, data acquisition and transmission capabilities, in situ video monitoring, temperature measurement and feed back control system in a closed loop operation[4-5].

Solid freeform fabrication using laser sintering generates parts by selective sintered multiple layers of powder to build a three dimensional part in layer-by-layer manner. The way to feed powder will not only effect productivity but also will effect the quality of sintered product. In this experimentation system, a piston feeding system is designed with which powder can be fed manually. Automatic powder feeding can also be done if electric motors are connected. After sintering, a new layer is lay down on top of the sintered one, then layer-by-layer is deposited to form a 3-D structure. Layer thickness ranges between 200 to 500 μm for various powders. The layers of powder is traced with a computer controlled laser scanning system (Fig. 1). The laser beam diameter is on the order of 700 μm, working output power ranges between 5 to 60 watts, diode laser has been used in the initial selective laser sintering (SLS) system. The laser beam rasters the powder bed surfaces and raises the temperature of the powder it contacts, sintering the loose powder. The laser scan rate is of the order of 1 ~2 cm/s for metals and ceramic powders @ 15 watts cw power. At the end of first scan second layer of loose powder is deposited as described earlier and the process is repeated. We have also designed an extra piston which is used to pressure the powder to the sintered layer each time when a new layer of powder is added on. This increases the compactness of spread out powder.

CAD data transferring

Most rapid prototyping processes produce parts on a layer-by-layer basis. The first step of the rapid prototyping is to slice the geometric description of the part (CAD data) into layers. The slicing operation generates the contours of the part for each layer (Fig. 1). Each layer then can be further divided into many scanning paths. Three scanning paths is currently under studies. They are raster scanning in a single direction, unidirectional scanning, directional scanning and contour scanning. Most current RP processes are using raster scanning in a single direction to build each layer of the part. Unidirectional scanning will result in a large number of very short scanning vectors which requires very precise and sensitive motor to control laser beam.

Directional scanning results in smaller number of longer vectors. Longer vectors reduce the errors associated with laser toggling transients and repositioning of the laser beam, resulting in higher part accuracy. Contour scanning of the layer boundaries is expected to generate better surface quality. The form of the geometric description of mechanical parts to be produced by sintering process significantly affects the accuracy of the final part. Most current technologies consists of tessellating the surfaces of the geometric model into a mesh of non-overlapping triangular facets. The resulting geometry is transmitted in a standard file format, the so-called "STL" file format, developed by 3D Systems, Inc. (1988)[3].This format has been adopted by many CAD vendors and is readily available.

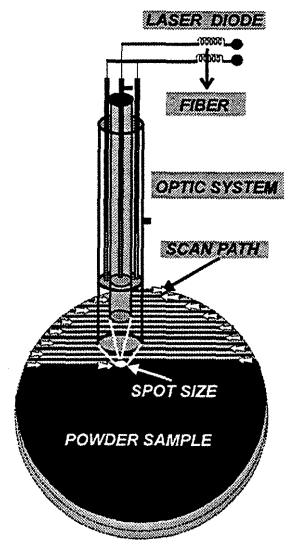

Fig.1 Computer Control Laser Scanning Path

Binding Mechanisms in SLS

Binding between powder particles takes place by laser induced localized heating. The duration of laser beam at any powder particle is short typically between 0.02 to 30 ms. Therefore the thermally-induced binding reactions must be kinetically rapid. Even at temperature approaching the melting point, metals and ceramics are very viscous and kinetic processes are very slow. For this reason, solid state binding mechanisms are not feasible for SFF technique. In SLS, the molten metal is often completely contained by loose powder rather than fully dense material. In this research we are developing two phase powder approach. In this approach the powder bed consists of two different powders of significantly disparate melting points. We are also working on the single phase powders sintering approach.

Computer Simulation

A distortion effect called "curl" is due to the material shrinkage force causing a bending moment perpendicular to the laser motion. As a result, mono-layers tend to bend horizontally from the test parts. Another effect responsible for part inaccuracies is the heat of polymerization evolving during the exothermal curing process. Mono layers tend to bend downwards on account of the inhomogeneous temperature distribution in their cross-section. The energy distribution of the laser spot on the surface of the powder sample is assumed to be Gaussian /Jacobs, with r being the Gaussian radius and where r may be a function of scanned time "t".

$$r = ((x(t) - x_0)^2 + (y(t) - y_0)^2)^{1/2}, \quad (1)$$

where x_o and y_o are the initial spot position.

Laser energy absorbed in the powder is given by the following equation:

$$dE/dz = eSE = -E_a; \quad (2)$$

where"e" being the absorptivity of the powder, "S" powder concentration and "E_a", is the energy absorbed by the powder. Computer simulation yields a deeper understanding of the physical, chemical and thermal processes occurring during SFF processes and are vital for an optimized finished 3-D part in terms of accuracy and quality.

MATERIALS

For SLS the materials used in the present study were Fe and Bronze-Fe and Bronze-Ni premixed powders. The powders were sieved and the particle sizes of the powders were 150 μm, 44 μm, 20 μm and 10 μm used in our experiment.

EXPERIMENTAL PROCEDURE

Several Bronze-Fe/Ni and Fe functional parts were made using SFF technique to determine the particle size effects and diode laser wave length effect on full density SLS parts. In this setup, the SFF device generates three-dimensional parts from CAD/CAM data files by selectively bonding multiple layers of powder using high-power diode lasers. For SFF requirements of the sintering experiments, the multi-mode fiber coupled power delivery system was attached with an optical re-imaging unit. The spot size of this unit using re-imaging unit is 700 ± 70 μm. Both of these systems can deliver intensity up to $1x10^4$ W/cm^2 at the powder bed.

Two Phase Sintering:

Two phase sintering during the SLS process in Bronze-Fe system occurs insitu liquid phase sintering (LPS) of low melting temperature alloy in a system. In the Bronze-Fe system, the melting temperature of iron is 1535^{O} C. In the temperature range between 870^{O} C and 1030^{O} C, the mushy bronze flows around the iron powders and forms a continuous substrate of bronze with an island of Fe powders. As the temperature increases by increasing the laser power or by decreasing the scan speed, the bronze powder becomes more liquid, viscosity decreases and liquid solid diffusion increases. This enhances the densifications of the SLS parts. For SLS parts the powder spread out density is around 30%. To increase the sinter density from 30% to fully dense there must be a mechanism to feed the powder in, unless there will be a shrinkage of the SLS parts or large zones of voids. To solve this problem, optimization of laser processing parameters and powder size and shape distribution is very important.

Single Phase Sintering:

At present we are also working on single phase sintering of powder. In this process melting of the powder is done by the laser beam. The melted zone moves continuously as the laser scans over the surface. As the molten zone moves, the solid-liquid reaction takes place. This process increases the density of the fabricated parts from 40% (spread out density) to more than 90%.

The strength and the surface finished of the sintered parts can be improved if the powder has the following properties:

1. **The particles must be well mixed and homogenized; particle size distribution within 10 μm.**
2. **The particle must not have any agglomerates and must be free of any contaminates.**
3. **The particle must have spherical morphology (equiaxed).**

Figs. 2 & 3 shows the SFF functional parts made from Fe-Bronze premix powders. Figs. 2a & 2b-3a is from 44 μm and 150 μm particle size powders respectively. Fig. 3b is from 44 μm particle size Fe powder. Three Fe-based samples were fabricated which has relatively high melting temperature of 1100^{O} C (Fig. 4). In addition two other Fe-based samples (Fig. 4) were sintered using two different laser radiations. The laser parameters for SLS were observed to be a power between 12 to 15 watts cw, a scan speed in between 1 to 2 mm/sec and a layer thickness of 250 μm. The depth of image plane on the powder bed is $\pm$100 μm for λ = 980 and 810 nm. For both the laser the spot size is about 700$\pm$70 μm. During SLS the powder bed temperature varies between $50^{O} \sim 100^{O}$C.

RESULTS

Some examples of preliminary SSF sintered parts with multiple sintered layers made from Fe/Ni-Bronze premix powders are shown in Figs. 2 & 3. It reveals that sintered part from finer particle size powder has more dense packing. Fig. 4 shows near net shape

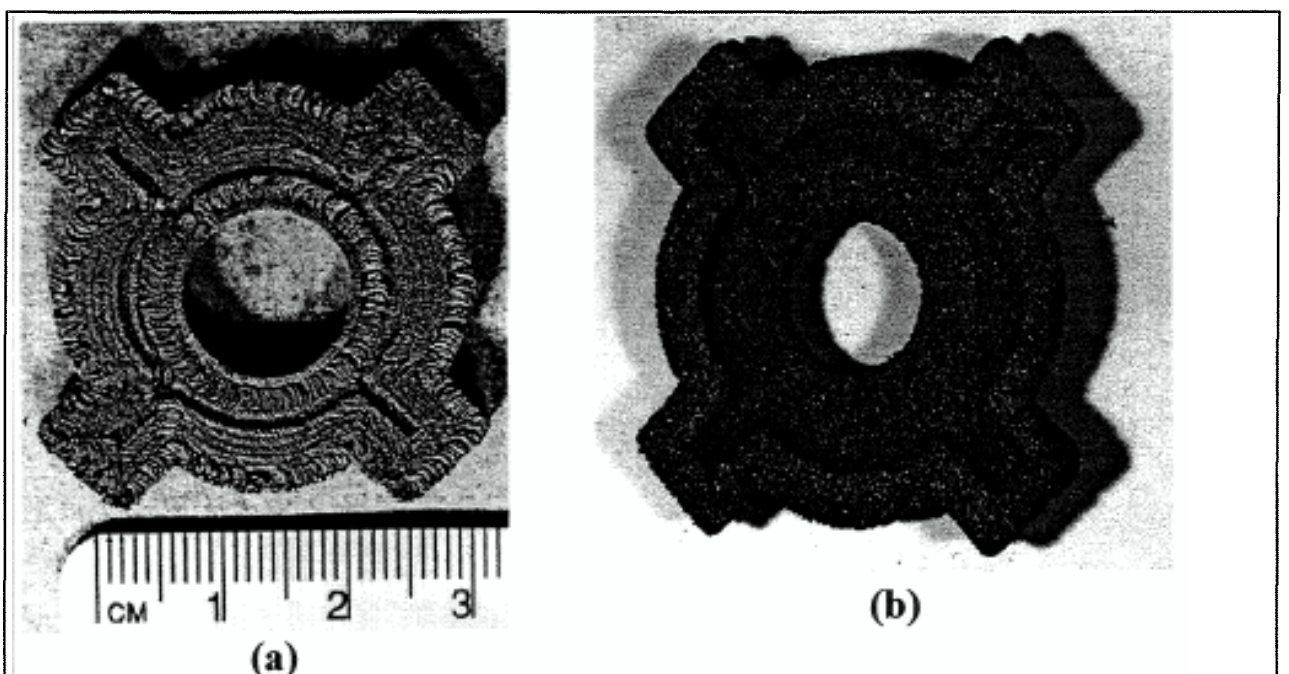

Figs. 2(a-b) The particle size effects of sintered samples made from iron-bronze premix powder in an argon atmosphere. As powder size decreases from left to right the resolution of SLS parts increases.
Figs. 2(a) Parameters used: λ = 980 nm, SS = 700$\pm$80 μm, SP = 1 mm/sec, Powder size = 44 μm, Power = 12 watts.
Fig. 2(b) Parameters used: λ = 980 nm, SS = 700$\pm$80 μm, SP = 1 mm/sec, Powder size = 150 μm, Power = 15 watts.

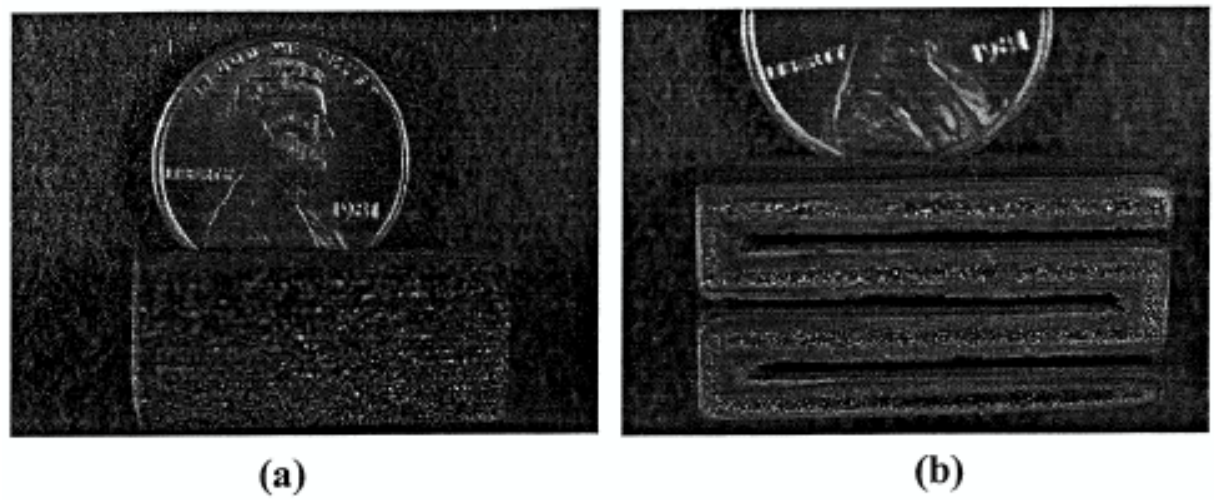

(a) (b)

Figs. 3(a-b) The wavelength effects of sintered samples made from iron/bronze premix powder and Fe powder in an argon atmosphere.
Fig. 3(a) Parameters used: λ = 810 nm, SS = 700$\pm$80 μm, SP = 1 mm/sec, Powder size = 150 μm Fe-Bronze, Power = 14 watts.
Fig. 3(b) Parameters used: λ = 980 nm, SS = 700$\pm$80 μm, SP = 1 mm/sec, Powder size = 150 μm Fe, Power = 14 watts.

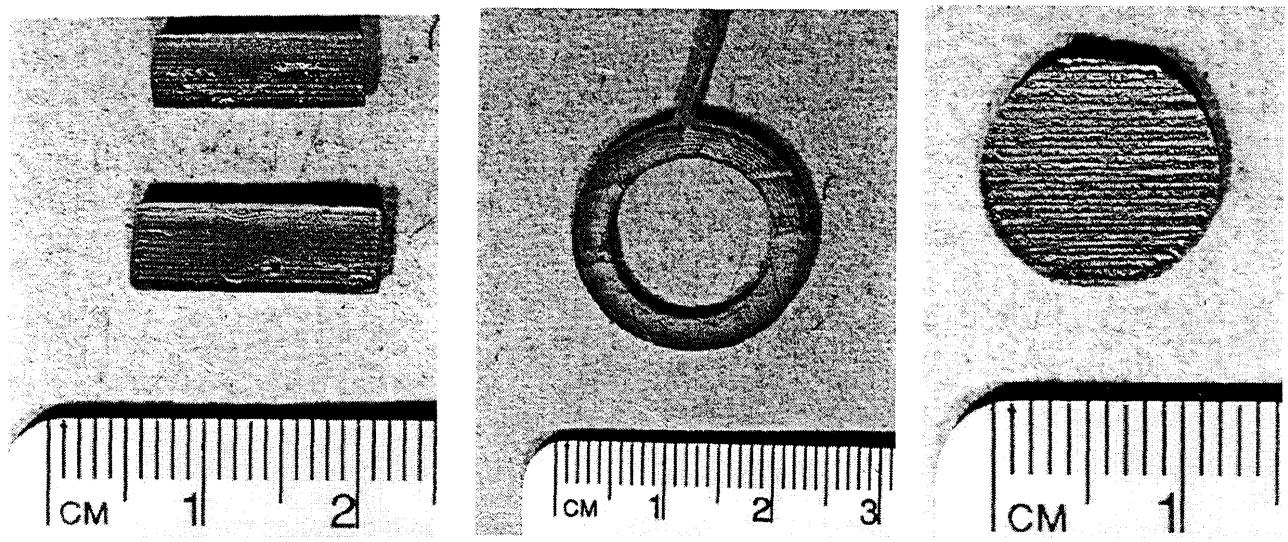

(a) (b) (c)

Figs. 4(a-c) The SFF Fe parts melted from 44 μm Fe powder using 810 nm diode laser. The laser spot size was 700$\pm$70 μm carrying 15 watts cw power at a 1 mm/sec scanning speed.

fully dense functional parts. The SFF parts were sintered from 44 μm Fe powder with the aid of 810 nm diode laser. The influence of laser radiation wavelength on quality of sintered parts was also studied. The results are shown in Figs. 3(b) & 4. As the laser wavelength decreases the laser radiation absorbed by the powder increases. Fig. 4 shows complete melting and sintered ring of Fe powder using 810 nm diode laser compared to partial melting and partial sintering of Fe powder (Fig. 3b) where 980 nm laser was used.

Density of SLS Parts

The sintered (Figs. 2 & 3) Fe-Bronze SLS parts made from 44 μm powder, have density of approximately 80% of the theoretical density compared to about 50% density of the 150 μm Fe-Bronze sintered SLS parts. SLS near net shape functional parts (Fig. 4) prepared from 44 μm iron powder using 810 nm diode laser have 90% of the theoretical density.

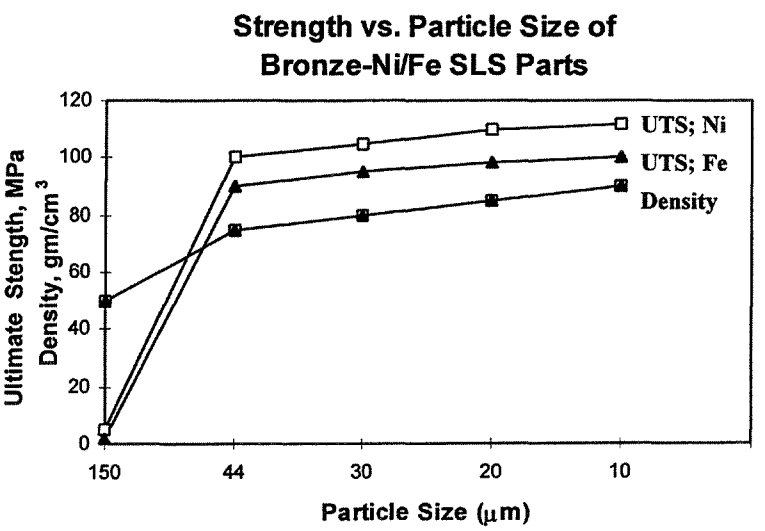

Fig. 5 Ultimate strength and density of Bronze-Ni/Fe powder as a function of particle size.

Strength of SLS Parts

Strength of SLS parts directly depends on the density or porosity. The dependency is similar to the profile which density exhibits with respect to processing parameters (laser scan speed, laser power, etc. Fig. 5). Fig. 5 shows an experimental result of ultimate strength as a function of particle size. From the figure it is evident that as the particle size of a powder decreases the ultimate strength of SLS parts increases. In Fig. 5 we have

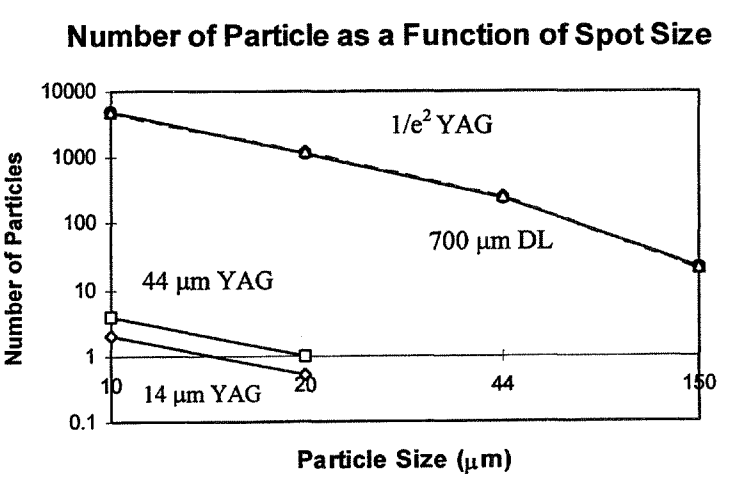

Fig. 6 Number of particles which can be accommodated within the spot area as a function of particle size.

also plotted density as a function of particle size. The density of SLS parts also increases as particle size decreases. Increase of pores reduce the load carrying capacity of the materials. Also pores or microcracks act as a site for stress concentrators for an effective crack's initiation site. Therefore, a SLS sample with density less than 100% is expected to have a strength less than that of a fully dense wrought material. Fractional density is also function of powder characteristics, such as particle size, size and shape distribution, etc. The following equation shows that strength is function of density:

$$\sigma = C\,\sigma_O\,f(\rho); \qquad (3)$$

where ρ is the fractional density of the SLS parts, σ is the strength and σ_O is the strength for the wrought material. In general,

$$\sigma = C\,\sigma_O\,\rho^m; \qquad (4)$$

where C and m are the material empirical constants for the material.

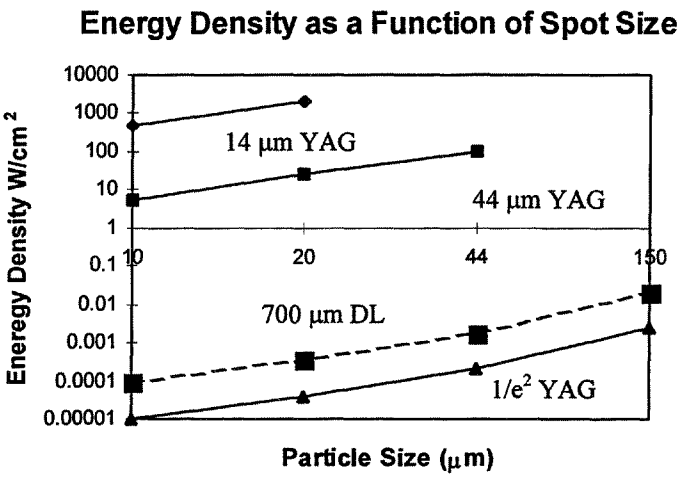

Fig. 7 Energy density per unit particle as a function of particle size

Curling of SLS Parts

In this research we did not observe any curling or bending of the Fe melted or sintered parts or any other Fe-Bronze sintered parts compared with the SLS parts fabricated by CO_2 or YAG lasers. Here we would like to address some of our findings of material photon interaction and their effects on materials properties. Fig. 6 is the calculated graph of total number of particles that can be accommodated inside an area. As the spot size decreases (14 μm YAG corresponds to 14 mm spot size at 10^7 W/cm^2 power density, 44 μm YAG corresponds to 44 μm spot size

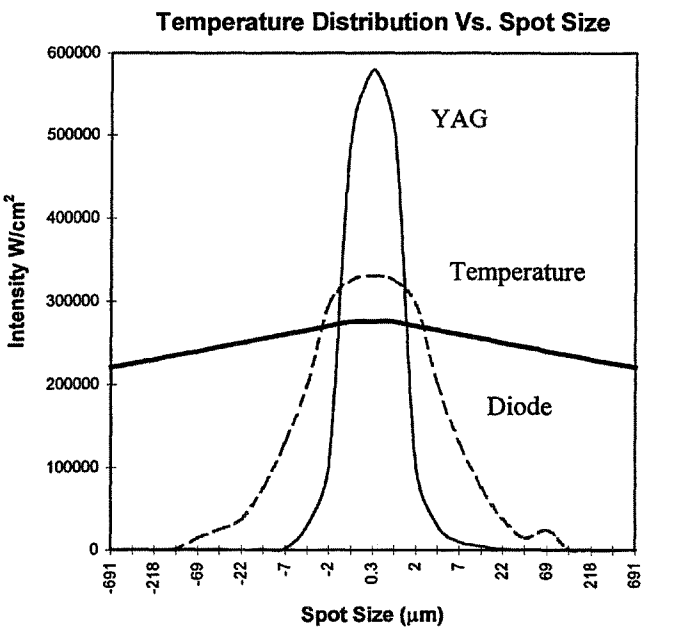

Fig. 8 Comparison of relative temperature distribution of YAG and diode laser as a function of a spot size.

at 10^6 W/cm^2 power density and 700 μm YAG corresponds to spot size at $1/e^2$ power density.), in case of an YAG laser the number of particles also decreases. The spread out powder particle density in an SLS process is about 30% of the calculated particle density. In Fig. 6 we also compared the spot size of a diode laser and the particle density. Fig. 7 is the calculated graph of an experimental value of an energy density. In this graph we are comparing the energy density per unit particle at different spot sizes. For YAG laser, energy density per particle increases as the spot size decreases. Fig. 8 is the relative comparison of temperature distribution of YAG and diode lasers. Diode laser having 700 μm spot size, is about 80% of its energy is within the spot area and just lies above the sintered temperature. If we compare the spot size of the YAG laser, the 80% energy corresponds to 44 μm spot size and the corresponding temperature is about twice higher. The large temperature gradient at the powder bed is the main cause of distortion of the sintered parts.

Energy Density

For a given power, density of the SLS Bronze-Fe parts increased as the scan speed and power size decreased. Also the density of the SLS parts is found to increase with increasing laser power for constant scan speed and power size. The higher density of the SLS part is achieved due to an increase of energy input to the per unit powder surface. The higher amount of energy per unit powder surface increases the temperature high enough to result in a large liquid phase formation of the low melting temperature alloy in two phase alloy systems. Bronze powder in a Bronze-Fe system melts incongruently between 870^O C (solidus) and 1030^O C (liquidus). A higher degree of liquid formation is observed as the temperature above the solidus increases. As the temperature increases the viscosity of the molten Bronze decreases which enhances the densification. However, at very high laser power and slow scan speed, significant amount of curling and warping phenomena was observed. Experiments had also been done to find the effect of the type of laser used to fabricate SLS parts. In this study diode (λ = 980 nm) and Nd:YAG (λ = 1060 nm) lasers had been used because both of them have very similar wavelengths. SLS parts fabricated using the YAG laser keeping all other parameters constant have shown significant amount of distortion and less densification compared to the parts fabricated by using the diode laser. There are two fold problems using the YAG laser. One is the wavelength disadvantage; YAG lasers have longer wavelength (1060 nm) compared to that of the diode lasers (810 nm). Which means that the diode laser energy is absorbed much more efficiently by the metallic powders compared to that of the YAG laser. Another one is the spot size disadvantage of the YAG laser over the diode laser. Due to this smaller spot size for YAG laser, powder particles are super-heated, and has large thermal gradient which is the main cause of the part's distortion. In this research we are using a new criterion to define usable energy delivered on per unit powder surface rather than per unit area on powder surface. Fig. 8 shows some temperature distribution of diode and YAG lasers with respect to sintered temperature. These new criteria will normalize the spot size effects between the two types of lasers. By optimizing the processing parameters it is possible to reduce the distortion.

MICROSTRUCTURE and QUALITATIVE MICRO-CHEMICAL ANALYSIS

To study the microstructure and to perform qualitative micro-chemical analysis of Fe-Bronze sintered samples, a scanning electron microscope (SEM), model Amray 1830I, with EDS capability was used. Energy dispersive x-ray spectroscopy (EDS) is a qualitative micro-chemical analysis technique with use of equipment attached to the SEM. The EDS analysis was used on different sintered samples to evaluate the degree of homogeneity also.

SFF samples from a coarser (Fe-Bronze) powder with the same power density and wavelength shows less homogenization than the samples prepared from finer powder. Figs. 9(a & c) show typical microstructures of sintered samples made from 150 μm and 44 μm Fe-Bronze powder, respectively. Figs. 9(b & d) are their corresponding EDS spectrogram. The two EDS spectrograms in Fig. 9b were obtained from two different areas of Fig. 9a. Area 1 in Fig. 9a shows mostly copper (Cu) with trace amount of iron (Fe). Areas 2 & 3 in Fig. 9a revealed similar results; mostly iron (Fe) with trace amount of copper (Cu). Fig. 9d shows two other EDS spectrograms obtained from Fig. 9c.

The spectrograms show that two different areas on the sample (Fig. 9c) has same amounts of Cu and Fe with a trace amount of Sn. The Cu-Sn phase diagram shows, prealloyed bronze powder with 6.97% Sn starts melting at around 800^{O} C. The complete melting of the system is at around 1000^{O} C. There is no existence of any binary or ternary phases in the Fe-Cu-Sn phase diagram. Comparisons of the spectrograms (Figs. 9b and 9d) reveal that finer powder shows more melting and homogenization compared to coarser pre-alloyed Fe-Bronze powder. In the coarse powder Fe and Cu stay separately.

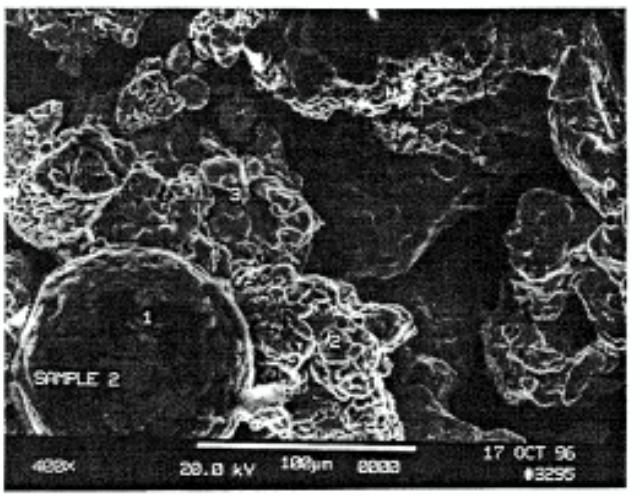

(a)

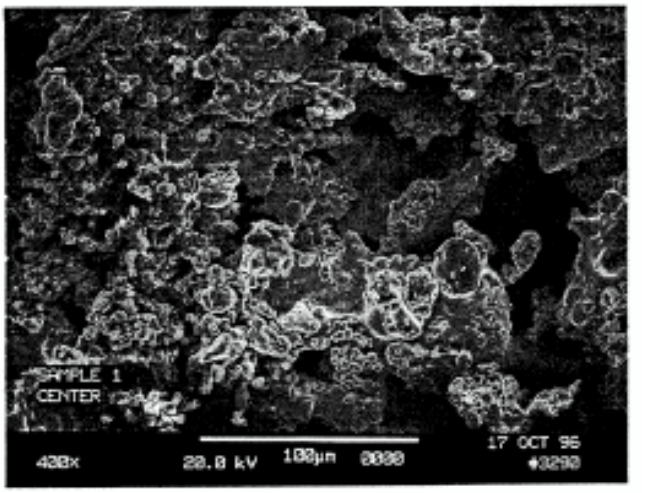

(c)

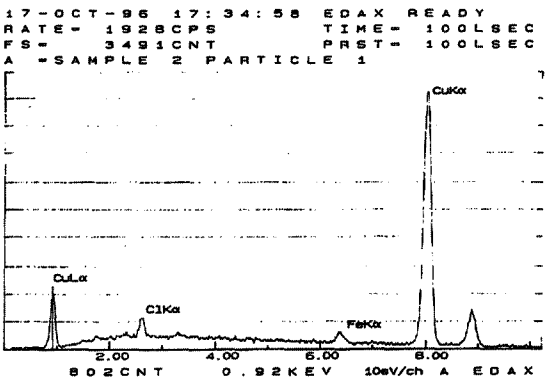

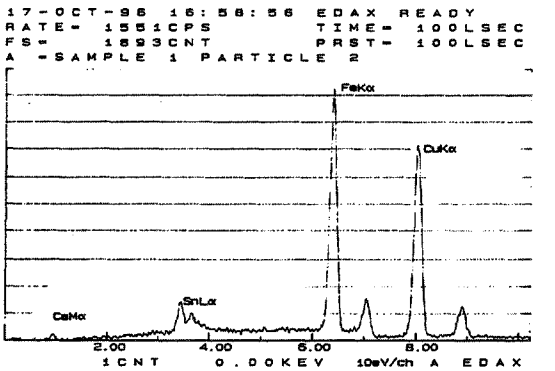

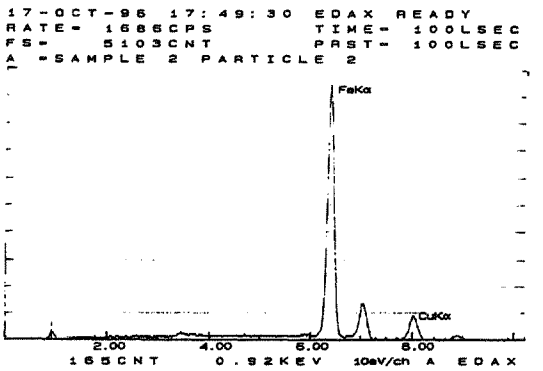

(b)

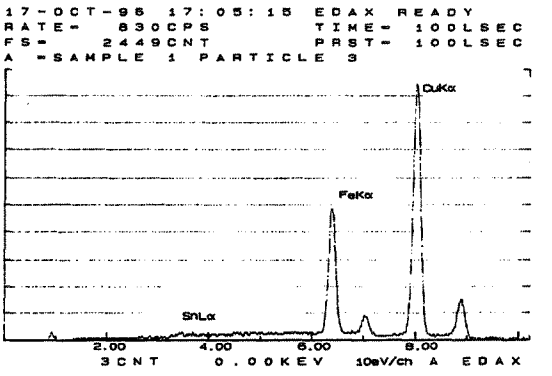

(d)

Fig. 9(a-d) is the SEM micrograph and EDAX of the Fe-Bronze premix powder at two different particle size.

Fig. 9(a) is the SEM micrograph of sintered Fe-Bronze parts. The powder size was 150 μm. Fig. 9(b) is the EDAX at two different particles of Fig. 9(a).

Fig. 9(c) is the SEM micrograph of sintered Fe-Bronze parts. The powder size was 44 μm. Fig. 9(d) is the EDAX at two different particles of Fig. 9(c).

OTHER RELATED WORKS

LASAMOCVD

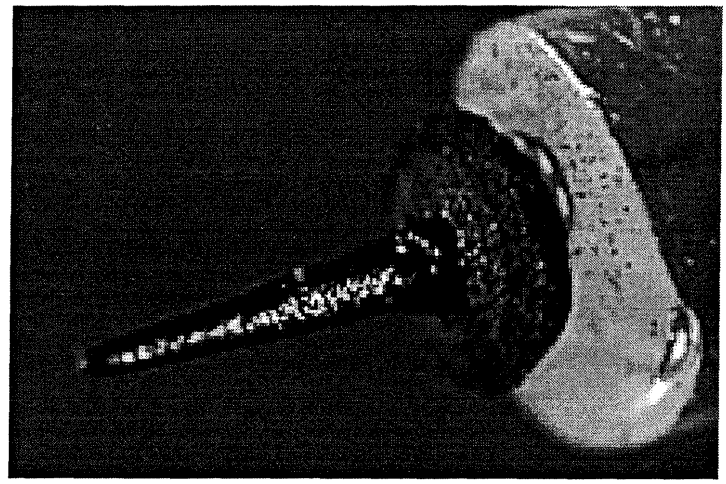

Fig. 10 SiC Rod Fabricated using LASAMOCVD techniques using diode laser, spot size = 600 μm, power cw = 12 watts, pressure = 25 torr TMS; time = 30 min, rod length = 10 mm, rod dia. at base = 700 μm and at top = 100 μm

Laser assisted selective area metal organic chemical vapor deposition (LASAMOCVD) is a locally controlled chemical vapor deposition (CVD) technique. There are two types LASAMOCVD, (1) pyrolytic and (2) photolytic. In pyroltic reaction, infrared diode laser beam interacts with the substrate to produce hot spot where thermally assisted chemical reactions take place. The film material is the decomposition product of the gas precursor. The film stick ton the substrate due to chemisorption processes. In the pyrolytic processes, the chemical reactions are usually takes place at the interface or just above the interface of the substrate. The selection of the precursors for LASAMOCVD is such that the decomposition temperature must be below the substrate melting temperature. The quality of the film or rod depends upon the precursor deposition temperature. Lower decomposition temperatures have a better film or rod quality. At DTM research lab at the University of Connecticut (Fig. 10), we had grown an amorphous and crystalline SiC, Si_3N_4 and graded SiC to Si_3N_4 rod of 1 to 2 mm diameter and 1 cm long. The volumetric deposition rate from $10^4 \sim 10^9$ micron/sec this corresponds to rod growth rate is of the order of mm/sec. For SiC rod fabrication, the gas precursor was tetramethylsilane (TMS) and for Si_3N_4, TMS and Ammonia (NH_4). Diode laser was used as a source of thermal energy for the decomposition of the gas. The solid decomposition products from the decomposition of the gas precursors by a laser beam in an atmospheric controlled chamber follow the laser beam profile. Therefore, the shape of the reaction products can be manipulated by beam steering, shaping, spot size controlling and beam scanning over the substrate on which deposition takes place. The decomposition of the gas takes place according to the following reactions:

For SiC: *Thermal Energy*

$$Si(CH_3)_4(g)[TMS] \xrightarrow{\text{Thermal Energy}} SiC(s) + 3CH_4$$

For Si_3N_4 *Thermal Energy*

$$3Si(CH_3)_4(g)[TMS] + 4NH_4\,[Ammonia] \xrightarrow{\text{Thermal Energy}} Si_3N_4 + 12CH_4 + 2H_2$$

Soldering

Laser beam soldered joints were made using Applied Optronics 30 watts cw (λ = 980 nm) fiber coupled diode laser, Fig. 11. The laser power and the soldering time were 7w and 1s, respectively. After soldering the joints were evaluated with binocular microscope to look for any damage or imperfections. Then a cross-section was cut and mounted in epoxy to facilitate optical microscope examination. No apparent damage was observed at a magnification of up to 500x. The microstructure and the wetting of the solder and substrate were good.

The microhardness of the bulk solder joint was measured using a knoop indentor, 20-gm load.

The values are:

Solder	Hardness Number
60Sn-40Pb	Knoop 18
97Sn-3Ag	Knoop 20

60Sn-40Pb (soft solder): The 60Sn-40Pb alloy has a two phase microstructure that consists of small dendrites of lead rich solid solution in a matrix of finer globular tin-lead eutectic. At a magnification of 500X there was no evidence of any intermetallic phase of Cu-Sn at the interface.

97Sn-3Ag: The microstructure consists of light color polygranular grains of tin-rich solid solution in a matrix of lamellar eutectic consisting of tin and Ag_3Sn intermetallic phase. There is no evidence of presence of any intermetallic phase of Cu-Sn in the microstructure. The micrographs revealed that there were no cracks, microcracks or pores present at the solder interfaces.

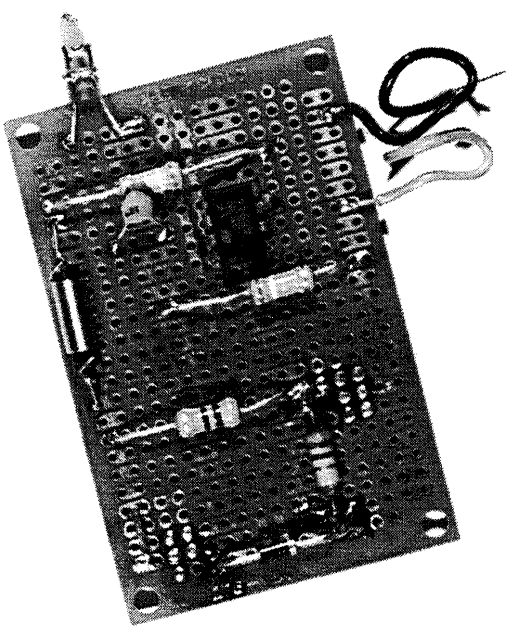

Fig. 11. High power diode laser soldering for electronic component assembly

Ultimate Breaking Strength (UBS)

The ultimate breaking strength for both the samples were measured. The samples failed from the substrate-solder interface. For Sn-Pb sample UBS was 730 lb/cm^2 and that for Sn-Ag was 790 lb/cm^2.

Depending upon the demands of electronics applications the lower melting temperature can accommodate larger amount of strain due to mechanical or thermal stress. However,

where the dimensionality and stability of the joint is important the higher melting solder is better.

Transformation Hardening

Fig. 12 shows microstructutes of the stainless steel (a) before and (b) after laser irradiation which demonstrates successful transformation hardening. The phase was transformed from pearlite to martensite, with increased hardness from 30 to 70 in Rockwell C scale.

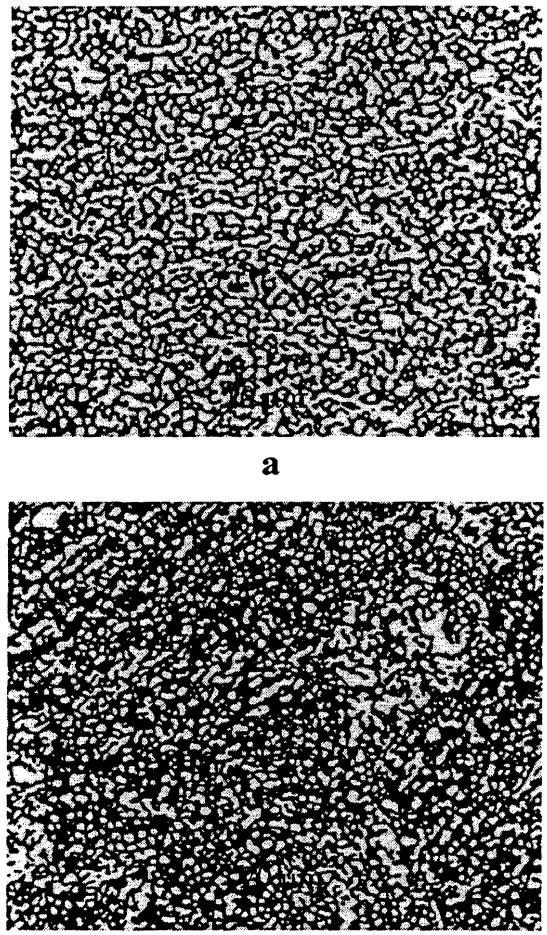

Fig.12 SEM micrograph of stainless steel: (a) before heat treatment, Pearlite phase; (b) after heat-treatment, Martensite phase[4]

CONCLUSION

The key success of DTM is the high brightness diode laser and to preserve this brightness when coupled to fiber delivery systems. At present all the commercial diodes use edge emitting technology edge emitting diode has high brightness of the order of 10^6 W/cm^2 at the facet but the coupling is very difficult. The commercial coupling underutilized both the cross section and the numerical aperture of the fiber, the brightness of the coupled power is significantly reduced compare to the original cluster. One high brightness approach is under development in our DTM laboratory, where our group has successfully demonstrated the useful intensity of the order of one to two orders of magnitude improvements. These approach uses one or two dimensional arrays of diode clusters and re-image it at fourrier transform plane to preserve the brightness of the individual clusters and then coupled it to a fiber[2]. Technique based on surface emitting distributed feedback (DFB) high brightness approach is under development at Hughes Danbury Optical Systems (Danbury, CT). At Hughes diode laser investigators have successfully demonstrated two orders of magnitude increase of useful intensity (10^6 W/cm^2) compare to current commercial technology (10^4 W/cm^2). At present our DTM lab has one such system. Power output of such diode laser has 10 watts cw into a spot size of 200 μm at 0.14 NA. By using 4:1 re-imaging unit we can reduce the spot size of the order of 50 μm at 0.5 NA.

Direct SLS of Bronze-Fe/Ni and Fe parts were studied by evaluating the density and microstructure of the parts as a function of processing parameters and powder size. We are particularly excited about our success with diode lasers in direct metal powder sintering, soldering, LASAMOCD for growing devices and other processes. The DTM technology will be capable of rapidly producing intricate, close-tolerance parts, a superior alternative to current prototyping techniques and in the near future will be used as a tool for rapid product development for desk-top manufacturing.

REFERENCES

1. Beam-material interaction spectrum, "Macro-materials processing". Proc. IEEE 70(6), 555-565(1982);C.M Banas and R. Webb.
2. Design Approaches for Laser-Diode Material-Processing Systems Using Fiber and Micro Optics; "Optical Engineering/Nov 1994/ Vol. 33, No. 11; W. Chen, Chandra Roychoudhuri.
3. "Solid Freeform Fabrication Symposium Proceedings 1990-95" Austin, Texas; Harris Marcus, David Bourell, Richard Crawford, Joel Barlow.
4. Potential Role of High power Laser Diode in Manufacturing, "SPIE Photonics West Conference", San Jose, Calofornia, Jan 27, 1996, pp 490/SPIE Vol. 2703; Tariq Manzur, Tony DeMaria, Weiquin Chen, Chandra Roychoudhuri.
5. SFF Using Diode Laser, "Solid Freeform Fabrication Symposium Proceedings 1996" Austin, Texas, pp 363-368; Tariq Manzur, Chandra Roychoudhuri, Harris Marcus.